

spheric ion irradiation. Magnetospheric ion densities are comparable to densities found near Europa and Ganymede (19). Thus, these satellites are good candidates for searches for O₃ absorption that will test the range of environmental conditions under which O₂-O₃ systems can be formed.

Bodies with icy surfaces are, by far, the most numerous objects in the solar system. Other planetary systems are also, probably, dominated by icy objects. Ganymede is a world with a diameter 40% the diameter of Earth where an abundance of O₃ has been produced, through an inorganic process, that is a not insignificant fraction of that in Earth's atmosphere. Searches for Earth-like planets harboring life similar to life on our planet that rely on the detection of O₃ (25) will have to take this process into account.

REFERENCES AND NOTES

1. J. R. Spencer, W. M. Calvin, M. J. Person, *J. Geophys. Res.* **100**, 19049 (1995).
2. W. H. Calvin, R. E. Johnson, J. R. Spencer, *Geophys. Res. Lett.* **23**, 673 (1996).
3. R. M. Nelson *et al.*, *Icarus* **72**, 358 (1987).
4. A. L. Lane, R. M. Nelson, D. L. Matson, *Nature* **292**, 38 (1981).
5. N. J. Sack, R. E. Johnson, J. W. Boring, R. A. Baragiola, *Icarus* **100**, 534 (1992). We use a density of 1.4 g cm⁻³ for SO₂ ice. The band at 280 nm observed for incident He⁺ is probably trapped OH and not O₂, as is suggested by Sack *et al.*
6. K. S. Noll, H. A. Weaver, A. M. Gonnella, *J. Geophys. Res.* **100**, 19057 (1995).
7. On both dates we observed through the G270H grating ($\lambda = 220$ to 330 nm) and the G190H grating ($\lambda = 155$ to 230 nm) for a total of 130 and 1080 s, respectively. All observations were made through the 0.86-arc sec-diameter circular aperture while the telescope tracked Ganymede. We used the blue digicon detector assay (FOS/BL); scattering within the grating dominated the detected signal at wavelengths below 210 nm. Ganymede was located with the Goddard High Resolution Spectrograph, after which we slewed to the FOS to make the observations. The expected precision of the final pointing is 0.1 arc sec. When we located Ganymede's trailing hemisphere, the final fine x-null balance was not completed, possibly because of bright, off-center albedo features. However, the ratio of trailing to leading hemisphere flux agrees with that found by IUE (3), indicating that the 0.86-arc sec aperture was filled by the 1.62-arc sec-diameter disk of Ganymede. We corrected the pipeline calibrated fluxes provided by the Space Telescope Science Institute to account for the fact that the angular size of Ganymede was larger than the aperture.
8. G. J. Rottman, private communication.
9. H. Taube, *Trans. Faraday Soc.* **53**, 656 (1956).
10. V. Vaida, D. J. Donaldson, S. J. Strickler, S. L. Stephens, J. W. Birks, *J. Phys. Chem.* **93**, 506 (1989).
11. D. G. Schleicher and M. F. A'Hearn, *Astrophys. J.* **331**, 1058 (1988).
12. A. J. Matich, M. G. Bakker, D. Lennon, T. I. Quickenden, C. G. Freeman, *J. Phys. Chem.* **97**, 10539 (1993).
13. A. J. Sedlacek and C. A. Wight, *ibid.* **93**, 509 (1989).
14. A. L. Lane, D. L. Domingue, S. K. Price, M. Lankton, *Bull. Am. Astron. Soc.* **26**, 1159 (1994).
15. N. J. Sack, J. W. Boring, R. E. Johnson, R. A. Baragiola, M. Shi, *J. Geophys. Res.* **96**, 17535 (1991).
16. The bracket notation is used to indicate number density. The ratio would be even larger if the shorter UV path length implied by the low UV albedo were taken into account. However, the estimate of the [O₃]/[O₂] ratio is uncertain by at least an order of magnitude, so

- additional refinements are unwarranted at this point.
17. A description of the Chapman reaction sequence can be found in J. W. Chamberlain and D. M. Hunten, *Theory of Planetary Atmospheres: An Introduction to Their Physics and Chemistry* (Academic Press, Orlando, FL, ed. 2, 1987). For the reaction $O + O_2 + M \rightarrow O_3 + M$, we use a rate $k_{12} = 6.0 \times 10^{-34}(T/300)^{-2.3} \text{ cm}^3 \text{ s}^{-1}$, or $4 \times 10^{-33} \text{ cm}^3 \text{ s}^{-1}$ for an assumed temperature T of 130 K. The reaction rate for $O + O_3 \rightarrow 2O_2$ is $k_{13} = 8.0 \times 10^{-12} e^{-2060/T} \text{ cm}^3 \text{ s}^{-1}$, which is $1 \times 10^{-18} \text{ cm}^3 \text{ s}^{-1}$ at 130 K. Photodissociation rates are affected by the extinction of UV flux in the ice layers. We used photodissociation rates for Earth's atmosphere at 60 km, where the overlying mass column abundance is roughly equivalent to a 1-cm-thick layer of ice, scaled by a factor of 0.074 to remove the diurnal variation and account for the reduced solar flux at Jupiter. For $O_2 + h\nu \rightarrow O + O$ (where $h\nu$ is the energy of a photon), we use the rate $J_2 = 4 \times 10^{-11} \text{ s}^{-1}$, and for $O_3 + h\nu \rightarrow O + O_2$, we use $J_3 = 3 \times 10^{-4} \text{ s}^{-1}$. The ratio J_2/J_3 is less sensitive to assumptions about UV extinction than are the individual rates. The Chapman reaction sequence is valid for gas-phase chemistry. Here we have used it to indicate high total densities that imply the O₂-O₃ system is located in high-density pockets within the surface ice. Thus, a full analysis of the chemistry will have to include reactions that take place on solid surfaces.
 18. A. L. Broadfoot *et al.*, *Science* **204**, 979 (1979). The value of [M] derived by our method, although highly uncertain, cannot be made to agree with the occultation upper limits even for extreme assumptions

about the possible uncertainty of [O₃]/[O₂].

19. R. E. Johnson, *Energetic Charged Particle Interactions with Atmospheres and Surfaces* (Springer, Berlin, 1990).
20. D. T. Hall, D. F. Strobel, P. D. Feldman, M. A. McGrath, H. A. Weaver, *Nature* **373**, 677 (1995).
21. F. Bagenal, D. E. Shemansky, R. L. McNutt Jr., R. Schreier, A. Eviatar, *Geophys. Res. Lett.* **19**, 79 (1992).
22. D. C. Hamilton, G. Gloeckler, S. M. Krimigis, L. J. Lanzerotti, *J. Geophys. Res.* **86**, 8301 (1981).
23. T. L. Roush, D. P. Cruikshank, T. C. Owen, in *Volatiles in the Earth and Solar System*, K. A. Farley, Ed. (American Institute of Physics, Washington, DC, 1995), pp. 143-153; R. N. Clark, R. H. Brown, P. D. Owensby, A. Steele, *Icarus* **58**, 265 (1984).
24. B. J. Buratti, J. A. Mosher, T. V. Johnson, *Icarus* **87**, 339 (1990).
25. B. F. Burke, *Nature* **322**, 340 (1986); A. Léger, M. Pirre, F. J. Marceau, *Astrophys. Space Sci.* **212**, 327 (1994); C. Sagan, W. R. Thompson, R. Carlson, D. Gurnett, C. Hord, *Nature* **365**, 715 (1993). Sagan *et al.* point out that the detection of disequilibrium O₃ is not, in itself, evidence of life.
26. We thank W. Calvin and J. Joiner for several enlightening discussions. These observations were supported by grant GO-5837 from the Space Telescope Science Institute, which is operated by the Association of Universities for Research in Astronomy under NASA contract NAS5-26555.

4 March 1996; accepted 29 May 1996

Self-Assembled Smectic Phases in Rod-Coil Block Copolymers

J. T. Chen, E. L. Thomas,* C. K. Ober,* G.-p. Mao

Rod-coil block copolymers are self-assembling polymers that combine the physics of orientational ordering of rodlike polymers and the microphase separation of coil-coil block copolymers. Several new solid-state morphologies were observed in a series of anionically synthesized model poly(hexyl isocyanate-*b*-styrene) rod-coil diblock copolymers examined by transmission electron microscopy and selected-area electron diffraction. The rod-coils formed smectic C-like and O-like morphologies with domain sizes ranging from tens of nanometers to almost 1 micrometer. Both structural and orientational changes were found for increasing rod volume fractions. In addition, some morphologies exhibited spontaneous long-range orientational order over many tens of micrometers.

In recent years, much work has focused on the morphology and phase behavior of block copolymers. The simplest copolymers are AB diblock copolymers, which are made up of two chemically distinct blocks covalently bonded together to form a single chain. Because of the mutual repulsion of dissimilar monomers and the constraint imposed by the connectivity of the A block with the B block, coil-coil diblocks (both blocks flexible) exhibit a wide range of

microphase-separated morphologies (1). The parameters that determine the morphology of a given block copolymer (2) are the Flory-Huggins interaction parameter, χ_{AB} ; the total degree of polymerization, $N = N_A + N_B$; and the volume fraction (composition) of the A component, f_A . The parameter χ_{AB} is a measure of the incompatibility between the A and B polymers and is inversely proportional to temperature.

Rodlike homopolymers have also been extensively studied. In contrast to flexible homopolymers, which obey Gaussian chain statistics and have persistence lengths of ~1 nm, rodlike polymers have nearly linear chain conformations and large persistence lengths ranging from 10 to 100 nm. The inherent chain stiffness of rodlike polymers

J. T. Chen and E. L. Thomas, Department of Materials Science and Engineering, Massachusetts Institute of Technology, Cambridge, MA 02139, USA.

C. K. Ober and G.-p. Mao, Department of Materials Science and Engineering, Cornell University, Ithaca, NY 14853, USA.

*To whom correspondence should be addressed.

causes them to form anisotropic liquid crystal (LC) phases in solution (3), in which the molecules are locally oriented along a preferred direction described by the director \hat{n} . The phase behavior of rodlike polymers can be controlled by either temperature (thermotropic) or solvent concentration (lyotropic).

Rod-coil diblock copolymers consisting of a rigid rod block and a flexible coil block represent a new class of self-assembling polymer. The morphologies of these materials arise from the competition between the microphase separation of the coil and rod blocks into mesoscopically ordered periodic structures and the tendency of the rod block to form anisotropic, orientationally ordered structures.

Morphological studies have been performed on rod-coil materials (4), but, with the exception of (5), none of the rod-coils studied had rod blocks that were both truly rigid and truly polymeric (a high degree of polymerization, N_{rod}). The anionically synthesized high-molecular-weight rod-coil diblock copolymer (see Fig. 1, A and B) reported in (5) combined a poly(hexyl isocyanate) (PHIC) rod block (weight average molecular weight M_w 58,000) and a polystyrene (PS) coil block (M_w 6600). Polarized optical microscopy (OM) studies of concentrated solutions in toluene confirmed LC ordering. Transmission electron microscopy (TEM) and selected-area electron diffraction (SAED) studies of solution-cast films revealed a zigzag lamellar (ZZ) morphology. Earlier investigators have studied the rodlike nature of PHIC in solution (6, 7) (the persistence length in a wide range of solvents is ~ 50 to 60 nm), the lyotropic behavior of PHIC in various solvents (8–10), and the crystal structure and helical conformation of PHIC in the solid state (5, 11).

We extended our synthesis of poly(hexyl isocyanate-*b*-styrene) [P(HIC-*b*-S)] rod-coil block copolymers, designated HS x / y , where x

is the M_w of the PHIC block and y is the M_w of the PS block in kilograms per mole (Table 1) (12), and have found evidence for two morphologies in addition to the ZZ morphology. OM studies of concentrated (>5% by weight) P(HIC-*b*-S) rod-coil-toluene solutions showed the formation of optically birefringent textures in all of the rod-coil solutions, which confirms the presence of nematic LC ordering on the molecular scale. The ability of the rod-coils to form orientationally ordered mesophases is not inhibited by the presence of the flexible PS coil block, even for HS73/104, which contains 58% PS by volume. The rodlike nature of the PHIC block plays a major role in the self-assembly of all of the rod-coil samples.

The rod-coil HS73/104, which has a coil block that is significantly larger than its rod block ($f_{\text{PHIC}} = 0.42$), forms a wavy lamellar structure consisting of discontinuous lens-shaped PHIC (lighter) domains surrounded by a continuous PS (darker) matrix (see Fig. 2A). The lighter domains, which have an average width of ~ 60 nm, were identified as the PHIC domains because they exhibited preferential mass loss during exposure to the electron beam (5). Unlike coil-coil diblock copolymers, rod-coils have substantial packing problems in the microphase-separated state. At the interface separating the rod and coil domains, the relatively smaller area per junction favored by the rod block results in chain stretching of the coil block, which is energetically unfavorable (13). Two ways of increasing the area per junction while maintaining constant density in the rod domains are to allow the rods to tilt and interdigitate. Given the PHIC M_w of 73,000 g/mol, the length of the rod block is predicted to be ~ 110 nm. If we assume interdigitation, the PHIC rods were tilted with respect to the lamellar normal by $\sim 60^\circ$. As a result, the wavy lamellar morphology (WL) resembles a smectic C phase. In addition, SAED patterns show that the

PHIC block is crystalline and that the local orientation of the PHIC chains extends over distances up to 1 μm . The lack of long-range orientational order may be due to reduced mobility of the rod-coils during microphase separation resulting from the entangled, high-viscosity PS block ($M_w = 104,000$).

Samples HS36/14 and HS58/7, which have rod blocks that are significantly larger than their low-molecular-weight coil blocks ($f_{\text{PHIC}} = 0.73$ and 0.90, respectively), form the second rod-coil morphology. Figures 2B and 2C show the ZZ morphology (5), which consists of alternating PHIC and PS layers arranged in a zigzag fashion. The rods in the ZZ morphology exhibit long-range orientational order (over several micrometers), which leads to the high degree of correlation observed between adjacent domains. The SAED patterns (see Fig. 2C, inset) confirm that the chain axis of the PHIC rods is tilted with respect to the lamellar normals by $\sim 45^\circ$ and that the PHIC domains are crystalline. Consequently, the ZZ morphology is also similar to a smectic C phase. The smaller tilt angle in comparison to the WL morphology is consistent with the reduced PS M_w and volume fraction (14). The formation of two distinct sets of lamellae with equal but opposite orientations from the local rod director is most likely a consequence of the nucleation of the smectic C phase in a thin film (if we assume that the director is in the plane of the film).

Low-dose serial images show that the lighter area located in the middle of the PHIC domain (for example, Fig. 2B) results from preferential mass loss due to beam damage. Because depolymerization is facilitated at the chain ends, this preferential location of the mass loss suggests a bilayer arrangement of the rods. Further evidence for a bilayer model is provided by atomic force microscopy images of both zigzag structures, which show a narrow groove that runs down the middle of the PHIC domain.

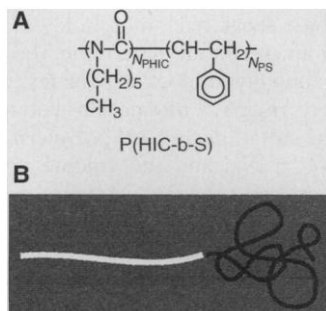


Fig. 1. (A) Chemical formula of the P(HIC-*b*-S) rod-coil diblock copolymer. PHIC is the rigid rod block, and PS is the flexible coil block. The N_{PHIC} and N_{PS} values for the samples studied are listed in Table 1. (B) Schematic drawing of the rod-coil molecule. The PHIC and PS blocks are depicted as a stiff rodlike chain and a Gaussian coil, respectively.

Table 1. List of the molecular weight characterization data for the HS x / y diblocks from GPC and NMR.

Sample	Total M_w^* (g/mol)	M_w/M_n	Molar ratio PHIC:PS	M_{PHIC}^\dagger (g/mol)	N_{PHIC}	f_{PHIC}	M_{PS}^\ddagger (g/mol)	N_{PS}	PS M_w/M_n
HS73/104	240,000	1.11	1:1.734	73,000	575	0.42	104,000	1000	1.05
HS36/14	68,000	1.40	1:0.477	36,000	283	0.73	14,000	135	1.04
HS58/7	222,000	1.86	1:0.138	58,000	457	0.90	6,600	63	1.08
HS245/9	1,819,000	2.52	1:0.046	245,000	1929	0.96	9,300	89	1.04
HS386/7	1,426,000	3.11	1:0.022	386,000	3039	0.98	7,100	68	1.04

*The total rod-coil M_w values and the number average molecular weight (M_n) values were determined relative to homoPS (Gaussian coil) standards. Because the hydrodynamic volume in solution has a stronger molecular weight dependence for a rod than for a coil, these values grossly overestimate the actual M_w values obtained by adding the PHIC (NMR) and PS (GPC) block M_w values separately. As a result, the tabulated values along with their corresponding polydispersities are useful only as a comparison between the various rod-coils. In addition, the uncertainty in the total M_w values for rod-coils HS245/9 and HS386/7 is greater because their apparent M_w values (>1,000,000 g/mol) are comparable to or greater than the highest molecular weight values resolvable by the GPC, given the distribution of pore sizes. † Values of M_{PHIC} were determined from the molar ratio obtained from NMR and the PS block M_w obtained from GPC. ‡ After polymerization of the PS block, a cannula was used to remove a 1-ml aliquot of the solution for GPC characterization.

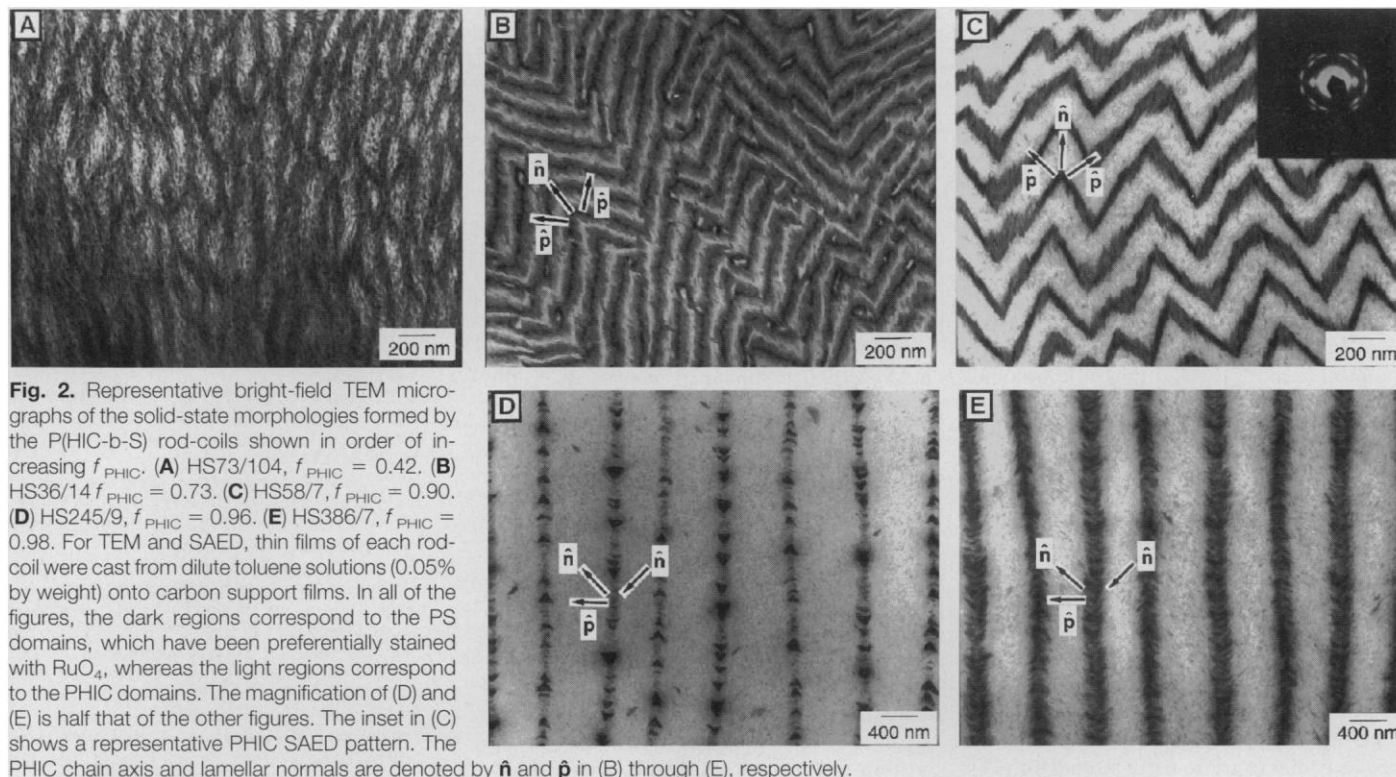


Fig. 2. Representative bright-field TEM micrographs of the solid-state morphologies formed by the P(HIC-b-S) rod-coils shown in order of increasing f_{PHIC} . (A) HS73/104, $f_{\text{PHIC}} = 0.42$. (B) HS36/14 $f_{\text{PHIC}} = 0.73$. (C) HS58/7, $f_{\text{PHIC}} = 0.90$. (D) HS245/9, $f_{\text{PHIC}} = 0.96$. (E) HS386/7, $f_{\text{PHIC}} = 0.98$. For TEM and SAED, thin films of each rod-coil were cast from dilute toluene solutions (0.05% by weight) onto carbon support films. In all of the figures, the dark regions correspond to the PS domains, which have been preferentially stained with RuO_4 , whereas the light regions correspond to the PHIC domains. The magnification of (D) and (E) is half that of the other figures. The inset in (C) shows a representative PHIC SAED pattern. The PHIC chain axis and lamellar normals are denoted by \hat{n} and \hat{p} in (B) through (E), respectively.

On the basis of a bilayer model, the predicted PHIC domain spacings parallel to the chain axis of 110 and 180 nm are found to be in good agreement with the average domain spacings measured from TEM of 120 and 190 nm, respectively (15).

The remaining rod-coils, HS245/9 and HS386/7, both of which have a short PS coil block and a very long PHIC rod block ($f_{\text{PHIC}} = 0.96$ and 0.98 , respectively), adopt a third alternating layer-type morphology. The morphology (Fig. 2, D and E) exhibits unprecedented long-range order over tens of micrometers in comparison to most self-assembling polymers. The PS block forms arrowhead (AH)-shaped domains whose ori-

entation flips by 180° between adjacent PS-rich layers. The SAED patterns, which show the superposition of two distinct single crystal-like PHIC patterns rotated relative to each other by an angle $\alpha \approx 90^\circ$, indicate that the orientation of the PHIC chain axis with respect to the layer normals in adjacent layers alternates between $\sim 45^\circ$ and -45° . This rod packing creates a chevron pattern whose orientation is commensurate with that of the PS arrowheads. The PS arrowheads are concentrated in the relatively narrow region separating adjacent PHIC domains where the local director abruptly changes its orientation (16). In terms of rod packing within the PHIC domains, a bilayer

model and an interdigitated model are found to be most consistent for HS245/9 and HS386/7, respectively. Given the PHIC block M_w values listed in Table 1 for HS245/9 and HS386/7, the predicted PHIC domain spacings (parallel to the chain axis) of 750 and 590 nm agree quite well with the average values obtained from TEM of 740 and 550 nm, respectively. In fact, given the difficulties involved in the M_w determination of high-molecular-weight rodlike polymers, molecular-weight values based on TEM measurements may offer a more accurate alternative.

Although a structure like the AH morphology has apparently not been observed in block copolymers, smectic mesophases in

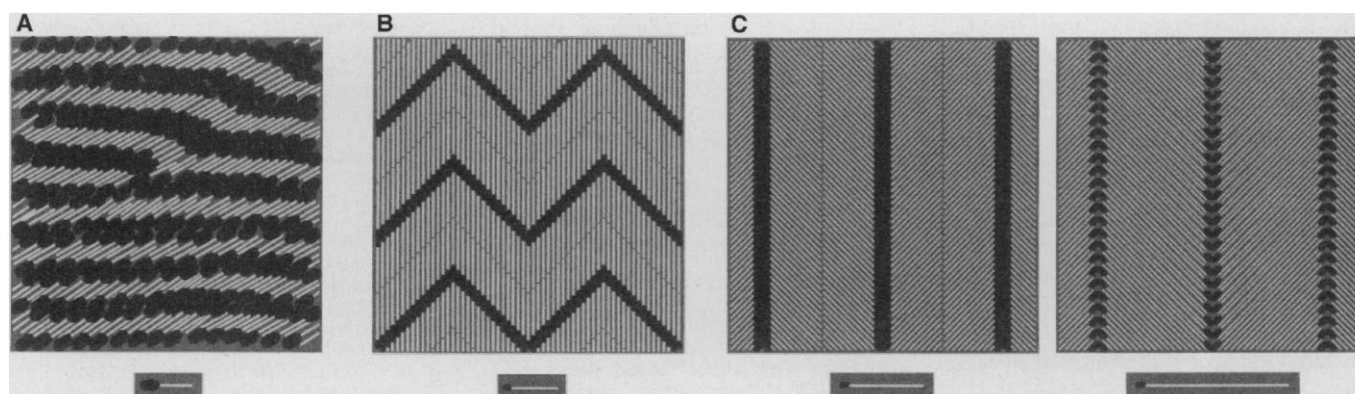


Fig. 3. Schematic models showing the packing arrangement of the rod-coil chains in the three solid-state morphologies. For a given rod-coil molecule, the PHIC block is represented by the white rod and the PS block by the black

ellipsoid. (A) WL morphology. (B) ZZ morphology. (C) Bilayer and interdigitated AH morphologies.

which the orientation of the director flips from layer to layer have been observed in small-molecule LCs (17–21). These mesophases were given the name smectic O. In particular, the smectic O structure was observed for racemic mixtures of chiral molecules (17, 21). Orientational phase transitions between the smectic O and the smectic C were observed with increasing temperature or applied electric field strength.

Schematic chain packing models of the WL, ZZ, and AH morphologies are illustrated in Fig. 3, A through C. Characteristics common to all of the rod-coil morphologies are a microphase-separated smectic-like layered structure and orientational ordering and tilting of the rods with respect to the layer normals.

The reasons for the formation of these self-assembled morphologies are by no means fully understood. In recent years, a number of theoretical predictions have been made about the phase behavior of rod-coil block copolymers (22–28). These predictions suggest a way by which the microphase-separated P(HIC-b-S) morphologies form. In coil-coil block copolymers, solvent concentration plays an analogous role to temperature by reducing χ_{AB} . From the isotropic state, lowering temperature or increasing block copolymer concentration by solvent evaporation results in microphase separation. For P(HIC-b-S), however, a competition exists between the onset of liquid crystallinity and microphase separation. Rod-coil theories have predicted that the isotropic solution will first form a homogeneously mixed nematic (with the rods orientationally ordered) before microphase separation. Eventually, the incompatibility of the rod and coil blocks drives the P(HIC-b-S) solutions to microphase-separate into the orientationally ordered smectic-like lamellar morphologies. When the solvent is completely removed, the PHIC domains crystallize and lock in the microphase-separated structures.

Although the above explanation is consistent with the observed LC and solid-state P(HIC-b-S) morphologies, the specific morphologies predicted by the earlier theoretical studies (22–28) are not observed. In particular, morphologies such as the monolayer and bilayer lamellar smectic A phases predicted by Semenov and Vasilenko (22) or the monolayer and bilayer “hockey-puck” phases predicted by Williams and Fredrickson to exist over much of the rod-rich portion of the phase diagram (27) are not observed in the P(HIC-b-S) rod-coil system. In addition, predictions by Semenov and Vasilenko that the tilted smectic C phase should exist for $f_{coil} > 0.64$ or the suggestion by Halperin (23, 24) that a smectic C phase is favored for high coil volume fractions are contrary to our exper-

imental findings. Furthermore, in earlier papers (22–28) the researchers did not specifically address rod-coil morphologies such as the ZZ or the AH morphologies.

A statistical theory recently developed by Gurovich (29) to treat the microphase separation of LC diblock copolymer melts near the spinodal is quite promising. In this work, the $\chi_{AB}N$ versus f_A phase diagram for an LC-coil diblock copolymer is predicted. The LC nature of the A block is treated in the theory through an orientational interaction that is approximated by a self-consistent molecular field. Although similar in many ways to the classical phase diagram of coil-coil diblock copolymers developed by Leibler (2), this LC-coil phase diagram exhibits several important differences. In particular, at a temperature above the order-disorder temperature, a disordered homogeneously mixed nematic melt is predicted for $f_{rod} > 0.27$. When cooled, the homogeneously mixed nematic undergoes microphase separation into a lamellar phase, ($0.27 < f_{rod} \leq 0.77$), and three new orientationally ordered lamellar phases that are separated by orientational phase transitions are predicted. The three phases in order of increasing f_{rod} are characterized by a local director that is oriented parallel (smectic A), tilted (smectic C), and perpendicular (no name) to the lamellar normal, respectively. Although Gurovich's theory is not strictly valid for rod-coil diblock copolymers, the WL, ZZ, and AH morphologies are more consistent with his phase diagram than with other proposed rod-coil phase diagrams (22, 27). In particular, tilted smectic C phases are predicted to exist over a large composition range, which qualitatively agrees with our observations. In addition, orientational phase transitions between different smectic phases, such as WL \leftrightarrow ZZ, are predicted as f_{rod} is varied. The ZZ \leftrightarrow AH phase transition, however, is a different type of orientational transition not predicted by Gurovich.

The phase behavior of microphase-separated rod-coil block copolymers is a rich and essentially unexplored area of research. Clearly, more work must be done before the multitude of solid-state morphologies are experimentally discovered and a rigorously valid theory that successfully explains the underlying physics of rod-coil self-assembly is developed.

REFERENCES AND NOTES

- G. H. Fredrickson and F. S. Bates, *Annu. Rev. Phys. Chem.* **41**, 525 (1990).
- L. Leibler, *Macromolecules* **13**, 1602 (1980).
- P. J. Flory, *Proc. R. Soc. London Ser. A* **243**, 73 (1956).
- Diblock and triblock rod-coil-(rod) studies are presented in the following references and discussed in (5): B. Perly, A. Douy, B. Gallot, *Makromol. Chem.* **177**, 2569 (1976); A. Douy and B. Gallot, *Polym. Eng. Sci.* **17**, 523 (1977); A. Nakajima, T. Hayashi, K. Kugo, K. Shinoda, *Macromolecules* **12**, 840 (1979); S. Barenberg, J. M. Anderson, P. H. Geil, *Int. J. Biol. Macromol.* **3**, 82 (1981); A. Douy and B. Gallot, *Polymer* **28**, 147 (1987); L. H. Radzilowski, J. L. Wu, S. I. Stupp, *Macromolecules* **26**, 879 (1993). An additional reference [L. H. Radzilowski and S. I. Stupp, *ibid.* **27**, 7747 (1994)] discusses coil-rich diblocks that were found to form morphologies ranging from alternating strips to discrete aggregates.
- J. T. Chen, E. L. Thomas, C. K. Ober, S. S. Hwang, *Macromolecules* **28**, 1688 (1995).
- M. N. Berger, *J. Macromol. Sci. Rev. Macromol. Chem.* **C9**, 269 (1973).
- A. J. Bur and L. J. Fetters, *Chem. Rev.* **76**, 727 (1976).
- S. M. Aharoni, *Macromolecules* **12**, 94 (1979).
- _____ and E. K. Walsh, *ibid.*, p. 271.
- S. M. Aharoni, *J. Polym. Sci. Polym. Phys. Ed.* **18**, 1439 (1980).
- S. B. Clough, in *Characterization of Materials in Research Ceramics and Polymers*, J. J. Burke and V. Weiss, Eds. (Syracuse Univ. Press, Syracuse, NY, 1975), pp. 417–436.
- We determined the molecular-weight characteristics and composition of each rod-coil using gel permeation chromatography (GPC) and ^1H nuclear magnetic resonance (NMR) spectroscopy.
- The area per junction for the PHIC rod is approximately 1 nm^2 and is independent of the M_w of the rod block. The area per junction for the PS coil varies (if strong segregation is assumed) with $M^{1/3}$. On the basis of data for strongly segregated lamellar diblocks of PS-polydiene, the area per chain varies as $0.14M^{1/3} \text{ nm}^2$, where M is the molecular weight of the PS block in grams per mole.
- The observed tilt angle of the PHIC is determined not only by the packing requirement in the LC state but also by crystallization of the PHIC chains, which necessitates axial registry of the chain axis repeat unit and leads to quantization of the tilt angle [see (5) for further discussion].
- In (5), Chen *et al.* found an interdigitated model to be most consistent with the PHIC domain spacing measured using TEM and with that based on the PHIC block M_w . Since then, the M_w of the PHIC block for HS58/7 has been determined more accurately. The revised bilayer PHIC domain spacing presented here is based on the improved M_w data.
- Given that the M_w of the PS block is quite similar for HS58/7, HS245/9, and HS386/7, it is not surprising that, locally, the chain packing at the rod-coil interface gives approximately the same tilt angle for the rod block with respect to the normal to the PS layer (or the row of PS arrowheads).
- A. M. Levelut, C. Germain, P. Keller, L. Liebert, *J. Phys. (Paris)* **44**, 623 (1983).
- A. D. L. Chandani, E. Gorecka, Y. Ouchi, H. Takezoe, A. Fukuda, *Jpn. J. Appl. Phys.* **28**, 1265 (1989). The mesophase studied in this work was similar to the smectic O; however, the investigators chose the nomenclature smectic C_A^* .
- Y. Galerme and L. Liebert, *Phys. Rev. Lett.* **64**, 906 (1990).
- _____, *ibid.* **66**, 2891 (1991).
- P. Hamelin, A. M. Levelut, P. Martinot-Lagarde, C. Germain, L. Liebert, *J. Phys. II (Paris)* **3**, 681 (1993).
- A. N. Semenov and S. V. Vasilenko, *Sov. Phys. JETP* **63**, 1 (1986).
- A. Halperin, *Europhys. Lett.* **10**, 549 (1989).
- _____, *Macromolecules* **23**, 2724 (1990).
- E. Raphael and P. G. de Gennes, *Physica A* **177**, 294 (1991).
- _____, *Makromol. Chem. Macromol. Symp.* **62**, 1 (1992).
- D. R. M. Williams and G. H. Fredrickson, *Macromolecules* **25**, 3561 (1992).
- R. Holyst and M. Schick, *J. Chem. Phys.* **26**, 730 (1992).
- E. Gurovich, *Macromolecules*, in press.
- Supported by NSF grants DMR92-14853 and DMR92-01845. We are grateful to E. Gurovich, A.-M. Levelut, and U. Breiner for useful discussions; to L. Fetters for doing the GPC, and to T. Mourey for additional M_w characterization of some of the rod-coils.

13 February 1996; accepted 13 May 1996